JB
Journals.ASM.org

Transposon Mutagenesis Identifies Uropathogenic *Escherichia coli* Biofilm Factors

Maria Hadjifrangiskou,[a]* Alice P. Gu,[b] Jerome S. Pinkner,[a,c] Maria Kostakioti,[a] Ellisa W. Zhang,[a] Sarah E. Greene,[a] and Scott J. Hultgren[a,c]

Department of Molecular Microbiology & Microbial Pathogenesis,[a] Center for Women's Infectious Disease Research,[c] Washington University in Saint Louis School of Medicine, St. Louis, Missouri, USA, and George Warren Brown School of Social Work, Washington University in Saint Louis, St. Louis, Missouri, USA[b]

Uropathogenic *Escherichia coli* (UPEC), which accounts for 85% of urinary tract infections (UTI), assembles biofilms in diverse environments, including the host. Besides forming biofilms on biotic surfaces and catheters, UPEC has evolved an intracellular pathogenic cascade that culminates in the formation of biofilm-like intracellular bacterial communities (IBCs) within bladder epithelial cells. Rapid bacterial replication during IBC formation augments a build-up in bacterial numbers and persistence within the host. Relatively little is known about factors mediating UPEC biofilm formation and how these overlap with IBC formation. To address this gap, we screened a UPEC transposon mutant library in three *in vitro* biofilm conditions: Luria broth (LB)-polyvinyl chloride (PVC), YESCA (yeast extract-Casamino Acids)-PVC, and YESCA-pellicle that are dependent on type 1 pili (LB) and curli (YESCA), respectively. Flagella are important in all three conditions. Mutants were identified that had biofilm defects in all three conditions but had no significant effects on the expression of type 1 pili, curli, or flagella. Thus, this approach uncovered a comprehensive inventory of novel effectors and regulators that are involved in UPEC biofilm formation under multiple conditions. A subset of these mutants was found to be dramatically attenuated and unable to form IBCs in a murine model of UTI. Collectively, this study expands our insights into UPEC multicellular behavior that may provide insights into IBC formation and virulence.

The orchestrated sequence of events that leads to biofilm formation encompasses reversible and irreversible stages that require conserved and species-specific factors regulated by hierarchically organized genetic networks (44, 51, 53). These regulatory systems respond to environmental cues to fine-tune the ordered transition from planktonic growth to biofilm by directing gene expression changes (41, 55, 56) and establishing developmental checkpoints, which once passed, commit cells to a specific fate (44). Biofilm-forming bacteria change their spatial and temporal organization (44) and alter the expression of surface molecules (41, 66), nutrient utilization and virulence factors (66), and resistance mechanisms to environmental stresses. In addition, the presence of environmental gradients within the biomass leads to community "division of labor" with subpopulations of bacteria exhibiting differential gene expression in response to local nutrient and oxygen availability (19, 42). Combined, these attributes confer a unique advantage to bacterial pathogens in biofilms and makes their eradication particularly difficult, resulting oftentimes in the establishment of chronic infections.

In the urinary tract, biofilm formation can lead to several serious infections, not only in catheterized patients but also in nonhospitalized individuals (21, 68). Eighty-five percent of community-acquired urinary tract infections (UTI) and 50% of device-associated UTI are caused by uropathogenic *Escherichia coli* (UPEC) (24), which employ a complex pathogenic cascade in the urinary tract, occupying extracellular and intracellular niches during the course of infection (60). UTI studies in mouse models have identified numerous virulence factors, including adhesins, toxins, iron acquisition systems, capsular structures, flagella, pathogenicity islands, and factors important for biofilm formation (3, 26, 28, 69–71). UPEC strains have genes that encode a multitude of chaperone/usher pathway (CUP) pili (14, 16, 35, 45, 64). The biogenesis, structure, and function of CUP pili have been extensively characterized (67). They typically contain adhesins at their tips that recognize specific receptors with stereochemical specificity (18, 30). For example, FimH, the type 1 pilus adhesin, binds mannosylated uroplakins, as well as N-linked oligosaccharides on β1 and α3 integrins that are expressed on the luminal surface of the bladder epithelium (urothelium) in mice and humans (20, 72, 73). Binding to the luminal surface of human bladder tissue *in situ* has been shown to be dependent on type 1 pili. Further, this binding can lead to bacterial internalization (12, 20, 30, 43, 62, 63, 73). Invading UPEC can be expelled from the host cell (10, 61), or they can "escape" into the cell cytoplasm. Within this intracellular niche, UPEC bacteria undergo a developmental process that culminates in the formation of biofilm-like intracellular bacterial communities (IBCs), comprising 10^4 to 10^5 tightly packed bacteria, which appear to be enclosed in an extracellular matrix (5, 31, 33). Polysaccharides, such as the sialic acid capsule, are also present throughout the IBC and function, in part, to protect the bacteria from neutrophil attack (3). Similar to extracellular biofilms, IBCs are heterogeneous and composed of subpopulations with different gene expression patterns (4). As IBCs enlarge, the eukaryotic cell volume becomes limiting, at which point UPEC cells

Received 6 June 2012 Accepted 29 August 2012
Published ahead of print 14 September 2012
Address correspondence to Scott J. Hultgren, hultgren@borcim.wustl.edu.
* Present address: Maria Hadjifrangiskou, Department of Pathology, Microbiology & Immunology, Vanderbilt University School of Medicine, Nashville, Tennessee, USA.
Supplemental material for this article may be found at http://jb.asm.org/.

doi:10.1128/JB.01012-12

alter their morphology, elongating and fluxing out of the host cell. These filamentous UPEC bacteria are capable of dispersing and reinitiating IBC formation in neighboring cells (31, 39).

One primary host defense that eliminates IBCs is exfoliation, where urothelial cells undergo an apoptosis-like cell death, detach from the underlying transitional epithelium, and are eliminated in the urine (46, 47, 50). Exfoliated bladder epithelial cells containing IBCs have been observed in urine collected from women with recurrent UTI, but not in healthy controls or in cases of UTI caused by Gram-positive pathogens (22, 57), demonstrating that observations from experimental murine infection models reflect human disease outcomes. However, exfoliation exposes underlying cell layers of the urothelium. Subsequent UPEC invasion of these underlying cells in mice results in the formation of additional intracellular structures termed quiescent intracellular reservoirs (QIRs) (47, 50). Mouse models have been used to demonstrate that bacteria in QIRs can contribute to recurrent infection after antibiotic treatment has rendered the urine sterile (46–48). Bacteria in the QIR are dormant, and studies have demonstrated that 17 different antibiotics capable of killing the virulent cystitis isolate UTI89 *in vitro* or in tissue culture, were unable to eliminate UTI89 from murine bladder tissue during bladder infection (11). These findings indicate that IBC and QIR formation constitute mechanisms that enable rapid bacterial expansion within a protected intracellular niche, shielded from host-mediated defenses and therapeutic interventions, such as antibiotic treatment. Thus, identifying factors that influence IBC formation either by impacting type 1 pilus expression or by an independent mechanism will advance our understanding of the regulatory systems that modulate UTI pathogenesis and will elucidate new targets for antivirulence therapy.

Few factors mediating IBC development have been identified thus far; studies have shown that type 1 pili are a critical IBC determinant, as interruption of *fim* expression after UPEC adherence and invasion of the bladder epithelium results in defects in IBC formation and loss of virulence (70). In addition to type 1 pili, sialic acid capsule has been implicated in IBC formation and UPEC virulence (3). Recent studies have identified the QseC sensor kinase as another IBC effector, as *qseC* deletion indirectly impacts expression of type 1 pili and interferes with biofilm formation (25, 37). Besides type 1 pili, deletion of *qseC* also impacts curli and flagella, two other critical UPEC biofilm determinants (37). Flagella have been extensively implicated in biofilm formation by *E. coli* (55), and several studies have shown that disruption of motility also influences *in vivo* UPEC virulence (39, 59, 71). Curli have also been shown to be important for *E. coli* biofilm formation in specific environmental niches, and studies have linked curli amyloid biogenesis to virulence (7, 15). Although the majority of *E. coli* and *Salmonella* strains produce curli optimally at 30°C or lower, many clinical UPEC and *E. coli* sepsis isolates express curli at 37°C (9, 32). Furthermore, Cegelski and Pinkner et al. demonstrated that low-molecular-weight inhibitors that disrupt curli biogenesis are efficacious in reducing bacterial colonization and IBC formation in a murine model of UTI (15), further linking curli formation to UPEC pathogenesis.

The identification of additional factors that are involved in IBC formation using large-scale *in vivo* screens has been difficult, partly due to population bottlenecks that arise during *in vivo* infection, which result in clonal IBC expansion (60). Given the biofilm-like properties of IBCs, we hypothesized that identification of biofilm effectors relevant in several *in vitro* conditions may provide insights into factors that contribute to fitness within the urinary tract, which would thus surmount the need for large-scale *in vivo* screening. Thus, we created a transposon mutant library in the virulent cystitis isolate UTI89, which we screened in three biofilm conditions: Luria broth (LB)-polyvinyl chloride (PVC), YESCA (yeast extract-Casamino Acids)-PVC, and YESCA-pellicle. These conditions were chosen, because they all depend on factors that are implicated in UTI virulence. LB-PVC biofilms are type 1 pili dependent, and YESCA-PVC and YESCA-pellicle biofilms are curli dependent. Flagella are important for biofilm formation in all 3 conditions. A total of 170 transposon (Tn) mutants with reproducible niche-specific or broad biofilm differences compared to wild-type (wt) UTI89 were identified. Of these, only the 40 mutants that had altered biofilm phenotypes (increased or reduced) under all conditions tested were considered for further study. They were all analyzed for type 1 pilus, curli, and flagellum expression in order to discern whether a given mutation identified potentially new requisites for UPEC biofilm formation. A panel of selected transposon mutants with disruptions in previously uncharacterized genes was found to be significantly attenuated in their ability to cause infection and form IBCs, indicating that at least some of these factors are also corequisites for IBC formation. Further characterization of these effectors will provide valuable insights into the mechanisms that underlie multicellular behavior and virulence in UPEC and will elucidate new targets for the development of antibiofilm agents.

MATERIALS AND METHODS

Bacterial strains and electrocompetent cells. UTI89 is a human cystitis isolate that is highly virulent in a mouse model of UTI (47). UTI89 was made electrocompetent after overnight growth in Luria broth (LB) medium lacking salt (no-salt LB) at 37°C with shaking. One milliliter of the overnight culture was used to inoculate 500 ml of prewarmed (37°C) no-salt LB and incubated aerobically at 37°C, with shaking until it reached an A_{600} of 0.6 to 0.75, at which point the culture was chilled on ice for 15 min. Bacterial cells were pelleted at 8,000 rpm for 10 min, washed 2 times, first in 75 ml of ice-cold 10% glycerol and then in 50 ml of ice-cold 10% glycerol, and resuspended in 1 ml of ice-cold 10% glycerol. The resulting electrocompetent cells had a transformation efficiency of 10^7 to 10^9 CFU/μg of DNA. Nonpolar gene deletions were performed using the λ Red recombinase method (49).

Transposon mutagenesis. Transposon mutagenesis was performed by electroporating 260 ng of the EZ-Tn5 <R6Kγori/KAN-2>Tnp Transposome kit (Epicentre) in 100 μl of UTI89 electrocompetent cells according to the manufacturer's instructions (Epicentre), followed by a 60-min recovery in SOC medium (0.5% yeast extract, 2% tryptone, 10 mM NaCl, 2.5 mM KCl, 10 mM $MgCl_2$, 10 mM $MgSO_4$, and 20 mM glucose) at 37°C. The entire transposition reaction was then diluted 1:10,000 and plated in 100-μl aliquots on LB-kanamycin plates to select for clones that contained a successful transposition event.

Transposition mapping. Transposon mutations were mapped using multiple-round PCR (6) and primer Inv-1 (ATGGCTCATAACACCCCTTGTATTA) or Inv-2 (GAACTTTTGCTGAGTTGAAGGATCA). The resulting amplicons were purified (Qiagen) and sequenced using the KAN-2 FP-1 forward and KAN-2 RP-1 reverse primers (Epicentre).

Biofilm assays. Transposon mutants were grown logarithmically in 3 ml LB and normalized to an optical density at 600 nm (OD_{600}) of 1. The cultures were then diluted 200-fold in fresh LB or yeast extract-Casamino Acids (YESCA) medium and used to seed biofilm plates. Biofilm assays in LB and YESCA media at room temperature were performed in 96-well PVC plates as previously described (54) and quantitatively measured 48 h postseeding, using crystal violet (52). Biofilm production for each mutant

A

Transposon library screening conditions			
Medium:	**LB**	**YESCA**	
Biofilm Type:	**Surface -associated**	**Surface -associated**	**Pellicle**
Temperature:	Room	Room	30°C
Format:	96-well	96-well	48-well
Score:	Colorimetric	Colorimetric	Visual
Known UPEC biofilm effectors:	Type 1 pili, flagella, QseC	Curli, flagella, QseC	Curli, flagella, Type 1 pili, siderophores, EPS, QseC
WT biofilm appearance (UTI89)	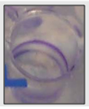		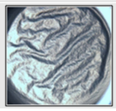

B

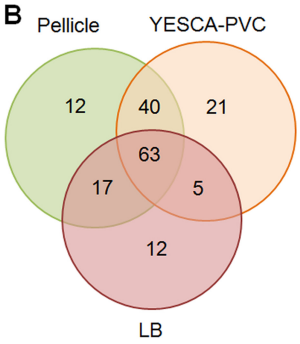

FIG 1 Transposon mutagenesis identifies mutants with broad and niche-specific biofilm defects in the virulent cystitis isolate UTI89. (A) Table depicting the three screening conditions used to identify transposon (Tn) mutants with biofilm defects and the expected biofilm appearance of the parent strain, wt UTI89. LB and YESCA-PVC biofilm assays were set up in 96-well PVC plates in either LB or yeast extract-Casamino Acids (YESCA) medium and incubated for 48 h at room temperature. Pellicle biofilm assays were set up in 48-well polystyrene plates in YESCA medium and incubated at 30°C for 48 h. Identified Tn mutants with biofilm defects were rescreened under all conditions three times. EPS, extracellular polymeric substance. (B) Venn diagram depicting the numbers of Tn mutants obtained that had biofilm defects in one or more of the initial biofilm screening conditions.

was normalized to the wt UTI89 OD_{565} reading, which was set at 100% for every run. Statistical analyses of three independent experiments were performed on all assays, using paired Student's *t* test ($P < 0.05$, considered significant). Pellicle formation assays in YESCA medium were performed in 48-well polystyrene plates at 30°C and qualitatively assessed at 48 h postseeding.

Motility assays. Motility assays were performed as previously described (71). Briefly, bacteria were incubated statically in LB for 18 h. Swimming was assessed in 0.25% LB agar–0.001% 2,3,5-triphenyltetrazolium chloride. The plates were incubated at 37°C for 7 h. Motility was evaluated by measuring the motility diameters. Experiment was repeated 5 times with triplicate plates for each strain.

HA assays. Bacteria were grown statically for 18 h and normalized to an OD_{600} of 1 in 1× phosphate-buffered saline (PBS). Hemagglutination (HA) assays were set up as described previously (29), using guinea pig red blood cells (RBCs) normalized to an OD_{640} of 2. For assessment of S-pilus-mediated adhesion, normalized RBCs were desialylated prior to the HA analysis as follows: normalized RBCs (OD_{640} of 2.0) were centrifuged at 3,000 rpm for 7 min, resuspended in 1 ml of 1× PBS, and incubated with slow rocking at 37°C for 2 h in the presence of 10 μl neuraminidase (50 mU; EY Labs)–100 mM sodium acetate (pH 5.5) or 10 μl of 100 mM sodium acetate (pH 5.5) (untreated control). At the end of the incubation period, the RBCs were centrifuged as described above to remove the enzyme and buffer, and the treated and untreated control RBCs were resuspended to an OD_{640} of 2.0 in 1× PBS.

Immunoblot analyses. For type 1 pili, cells were grown statically in LB for 18 h at 37°C and normalized to an OD_{600} of 1. Prior to processing for SDS-PAGE, samples were treated with 1 M HCl to dissociate pilin subunits, boiled for 5 min, and neutralized with 1 M NaOH prior to electrophoresis. Membranes were probed with antisera raised against type 1 pili (54) at a 1:3,000 dilution.

Mouse infections. Female C3H/HeN mice (Harlan) that were 7 to 9 weeks old were transurethrally infected with 10^7 CFU of isolate UTI89 carrying the green fluorescent protein (GFP)-expressing plasmid pANT4 (17) by the method of Hannan et al. (26). pANT4 is stably harbored by UPEC during the acute infection stages (31). Experiments were repeated 3 times, and statistical analyses were performed using the Mann-Whitney test (two-tailed). A *P* of <0.01 was considered significant. All procedures involving mice were performed in compliance with current federal guidelines and the institutional policies of the Washington University in Saint Louis and ensured proper and humane treatment of animals.

Microscopy. Bladders excised from infected animals were treated for confocal microscopy as previously described for IBC enumeration (71). Briefly, the bladders were bisected, splayed, and fixed in 4% paraformaldehyde overnight at 4°C. The fixed bladders were washed and counterstained for 20 min with the nuclear ToPro3 (Molecular Probes) stain, and recombinant wheat germ agglutinin (r-WGA) to outline the facet cells (1:700 dilution for each). Five bladders per mutant tested were scanned per experiment. Images were obtained using a Zeiss LSM 510 Meta Laser Scanning inverted confocal microscope (Thornwood). The average numbers of IBCs quantified in 3 independent experiments are reported. Statistical analyses were performed using a two-tailed Mann-Whitney test, with a *P* of <0.01 considered significant.

RESULTS AND DISCUSSION

An *in vitro* transposon screen identifies UPEC biofilm effectors. We generated a transposon library in the prototypic cystitis isolate UTI89, using the EZ-Tn5 <R6K*gori*/KAN-2>Tnp "transposome" (23). Of the 44,386 transposon mutants obtained using this method, we were able to manually screen 6,144 (1× coverage) for defects in three different biofilm conditions that are dependent on three factors that are implicated in UPEC virulence to different degrees: surface-associated biofilm on the walls of polyvinyl chloride (PVC) plates during static growth in room temperature LB (type 1 pili dependent) or YESCA broth (curli dependent) and floating pellicle biofilm formation during static growth in YESCA broth at 30°C (curli dependent) (Fig. 1A). In addition to type 1 pili and curli being critical determinants in the LB and YESCA biofilm assays, respectively, flagellum formation is also known to be important in all three biofilm conditions. Biofilm formation on the walls of PVC plates was measured at 48 h postinoculation using the crystal violet colorimetric method of O'Toole et al. (52) and normalized to values obtained for wild-type (wt) UTI89. The formation of floating pellicle biofilms on the liquid-air interface of YESCA broth at 30°C was scored visually, given a score of 0 to 4, with 4 being wt and 0 being "no pellicle" (see also Table S2 in the supplemental material).

Our initial screen identified a total of 234 biofilm mutants with altered biofilm properties in one or more of the conditions tested. Of the 234 mutants, 55 gave false-positive results and were discarded and 9 could not be maintained in culture, leaving a total of 170 transposon (Tn) mutants with consistently reproducible niche-specific or broad biofilm differences compared to the wt

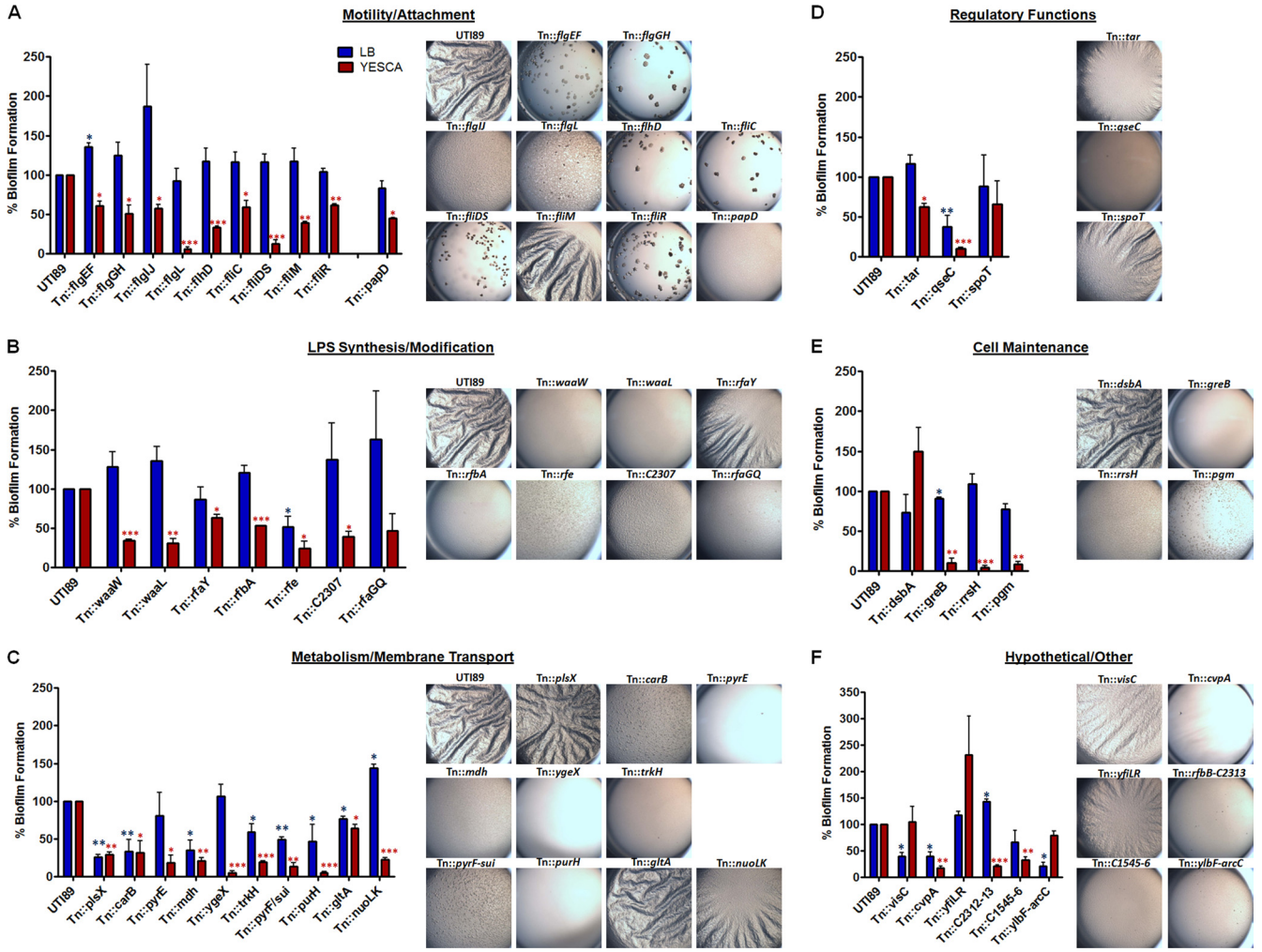

FIG 2 Functional classification of broad biofilm effectors. (A to F) Bar graphs showing the percent reduction or increase in biofilm formation on PVC plates by the different Tn mutants compared to wt UTI89 during growth in LB or YESCA. Biofilm production for each mutant was normalized to the wt UTI89 OD_{565} reading, which was set at 100%. Data shown are averages of 3 different independent experiments. Statistical analyses were performed using paired Student's *t* test (*, $P < 0.05$; **, $P < 0.005$; ***, $P < 0.0003$; blue asterisks denote significance for LB biofilm, red asterisks denote significance for YESCA biofilm relative to wt UTI89). Photo panels accompanying each graph depict the appearance of pellicle biofilm produced in polystyrene plates by each Tn mutant after 48 h of growth in YESCA medium at 30°C. Representative photos from 3 different experiments are shown.

UTI89 isolate (Fig. 1B; see Table S1 in the supplemental material). Of these, a total of 63 mutants exhibited altered biofilm characteristics in all three conditions tested. These mutants with broad biofilm alterations were selected for further analysis after validating that the biofilm defects observed for each mutant were not attributed to significant growth defects (data not shown). Using nested PCR and a combination of transposon-specific primers, we were able to map 54 of the 63 transposition events, identifying 40 chromosomal loci with nonpolar or polar gene disruptions (Table S2). Functional analysis classified the 40 biofilm-related genes in 6 general categories, encompassing motility/attachment, LPS synthesis/modification, metabolism and cell maintenance, as well as regulatory or hypothetical functions (Fig. 2). Mutants with the most significant quantifiable differences in biomass belonged to the metabolism and hypothetical function group (Fig. 2C and F), while mutants with more dramatic architectural differences belonged to the motility/attachment and lipopolysaccharide (LPS) synthesis modification groups (Fig. 2A and B; see Fig. S1 in the supplemental material). To validate our observations, we selected a panel of transposon mutations from the LPS synthesis/modification, metabolism and hypothetical function groups, which disrupted novel biofilm effectors (Tn::C3813-*purH*, Tn::*cvpA*, Tn::*plsX*, Tn::*carB*, Tn::*visC*, and Tn::*rfe*) and created clean, nonpolar deletions in isolate UTI89, which we tested for their biofilm properties in LB-PVC and YESCA-PVC. Indeed, all mutants exhibited similar phenotypes, as those exhibited by the corresponding Tn mutants (Fig. S2). These analyses also demonstrated that in the case of Tn::C3813-*purH*, the biofilm defect was attributed to *purH* disruption, as deletion of UTI89_C3813 imparted no biofilm defects, while the UTI89Δ*purH* strain exhibited a biofilm phenotype identical to that of the bacteria with Tn::C3813-*purH* (Fig. S2). In future studies, we will be generating clean gene deletions for each factor identified in our screen to determine polar effects and further characterize the contribution of each factor to UPEC biofilm formation.

Assessment of type 1 pilus, curli, and flagellum production in mutants with generalized biofilm defects. Type 1 pili, curli, and

flagella are key niche-specific determinants of the three biofilm conditions we used for our transposon library screening (Fig. 1A). Although mutations in the *fim* operon encoding type 1 pili abolish LB-PVC biofilms, they were not found to significantly affect YESCA-PVC biofilms. Accordingly, of the 170 transposon mutants with consistently reproducible niche-specific or broad biofilm differences compared to wt UTI89, 12 were in the *fim* operon and disrupted type 1 pili, impacting biofilm formation in LB-PVC and pellicle (2/3 conditions tested [see Table S1 in the supplemental material]). Mutant strains with mutations in *fim* while defective in LB biofilms still produce YESCA biofilms. Similarly, we identified 2 Tn mutants with disruptions in the *csg* operons encoding curli, and these abolished YESCA, but not LB PVC, biofilms (see Table S1 in the supplemental material). Thus, mutations in the *fim* and *csg* operons were not analyzed further in this study, as we carried through only the 40 mutants that had defects in all 3 biofilm conditions tested. However, since type 1 pili, curli, and flagella have known contributions to the various three biofilm conditions tested, we investigated the impact of each of these 43 mutations on the expression of each of these organelles in order to assess the novelty of the mutation versus a secondary effect on one of these known factors.

(i) Swimming motility. We assessed swimming motility on soft agar plates (0.03%) for each mutant, compared to the wt UTI89 isolate, over a 7-h incubation period. In this assay, the 9 nonmotile mutants disrupted for flagellar assembly or regulation (22.5% of the total [see Fig. S1 in the supplemental material]) served as controls (Fig. 3A). Of the remaining 31 Tn mutants tested, 2 exhibited increased motility (Tn::*rfaGQ* and Tn::*ylbF-arcC* [Fig. 3]), while 13 exhibited reduced motility. These reduced motility mutants were the Tn::*rfe* (LPS [Fig. 3B)]; Tn::*pyrE*, Tn::*mdh*, Tn::*trkH*, Tn::*pyrF-sui*, and Tn::*nuoLK* (metabolism [Fig. 3C]); Tn::*tar*, Tn::*qseC*, and Tn::*spoT* (regulators [Fig. 3D]); Tn::*greB* and Tn::*pgm* (cell maintenance [Fig. 3E]); and Tn::*visC* and Tn::*yfiLR* (hypothetical/other [Fig. 3F]) mutants. We have previously reported that deletion of *qseC* results in downregulation of motility by reducing the expression of *flhDC*. Similar analysis on the clean *visC* deletion mutant demonstrated no significant changes in *flhDC* or *fliC* expression (data not shown), suggesting that the effect on motility in this mutant occurs at the posttranscriptional level. We are currently studying the cause of the loss of motility in the nonmotile biofilm mutants. Taken together, the swimming motility assays indicate that approximately 50% of mutants with biofilm defects did not impact motility, suggesting that the corresponding factors influence biofilm formation by affecting an alternate pathway.

(ii) Type 1 pili. Next, we measured type 1 piliation by the ability of each mutant to mediate mannose-sensitive hemagglutination (MS-HA) (29). Expression of type 1 pili can be evaluated by the ability of UPEC to agglutinate guinea pig red blood cells (RBCs) via recognition of mannosylated receptors by the FimH adhesin. Type 1 piliated UTI89 typically produces an HA titer ($\log_2$) of 8 to 9 (29). The addition of mannose competitively inhibits type 1 pilus-mediated adhesion. Under the conditions tested, wt UTI89 typically expresses primarily type 1 pili. The addition of soluble D-mannose (2%) inhibits the HA reaction by competitively binding FimH and blocking bacterial binding to the mannosylated erythrocytes, thereby reducing the HA titer to 0 or 1 (29). The expression of other pilus systems can mediate hemagglutination that is mannose-resistant HA (MR-HA) (37). We thus used HAs in the presence and absence of D-mannose to assess the effects of each Tn mutation on expression of type 1 (MS-HA) and other adhesins (MR-HA). We detected significant reduction in type 1 pilus-mediated HA in only 8/40 mutants (20%), with the Tn::*mdh*, Tn::*qseC*, Tn::*visC*, and Tn::*ylbF-arcC* mutants exhibiting the most significant defects (HA < 7 [Fig. 4]). Interestingly, the Tn::*qseC*, Tn::*mdh*, and Tn::*visC* mutants were also defective in motility, a surprising observation given that motility and type 1 pilus expression are typically inversely related (40). We are currently investigating this phenomenon. In order to validate the HA results, we performed Western blot analyses on a subset of Tn mutants with different HA titers (Tn::*visC*, Tn::*rfe*, Tn::*yfiLR*, Tn::2312, Tn::C1545, and Tn::*ylbF-arcC*), probing for the major pilus subunit, FimA. Indeed, FimA protein levels in each mutant corresponded to the recorded HA (see Fig. S3 in the supplemental material), with the Tn::*visC* and Tn::*ylbF-arcC* mutants producing miniscule amounts of FimA, while the Tn::*rfe*, Tn::*yfiLR*, and Tn::C1545 mutants produced wt levels of FimA protein (Fig. S3). Numerous regulatory factors control expression of type 1 pili, including three major recombinases that alter the orientation of the invertible *fim* promoter element (1, 2, 13, 34). It is possible that disruption of *visC* and *ylbF-arcC* impact expression and/or function of regulatory elements, thus affecting the phase variation of the *fim* promoter, or *fim* gene transcription. Future studies are aimed at addressing these possibilities.

Interestingly, our HA analyses revealed that 18 mutants (45% of all mutants) had induced slight to moderate MR-HA (Fig. 4; see Table S1 in the supplemental material), indicative of induction of other adhesive organelles besides type 1 pili. We have previously shown that in the absence of the *qseC* sensor kinase, the observed MR-HA is attributed to upregulation of S-pili (25, 37) To examine whether S-pili were responsible for the induced MR-HA in the Tn mutants with MR-HA, we assessed HA, using RBCs treated with *Arthrobacter ureafaciens* neuraminidase to remove sialic acid, the putative receptor of S-pili (36). Desialylation of RBCs should abolish binding via S-pili, thus reducing the MR-HA to 0 or 1, unless other CUPs or adhesins are responsible for the observed MR-HA. Our assay revealed that in 16 out of the 18 mutants with MR-HA, desialylation of RBCs abolished MR-HA (see Fig. S4 in the supplemental material), indicating that disruption of the corresponding factors somehow induces the upregulation of S-pili. The 2 Tn mutants (Tn::*rrsH* and Tn::*rfe* mutants) that continued to exhibit MR-HA in the absence of sialic acid may have other adhesins that are upregulated or unmasked upon disruption of these factors, similar to what has previously been described (8, 27, 58, 65).

(iii) Curli. The ability of the different Tn mutants to form curli was evaluated on YESCA agar plates, using Congo red (CR) uptake as a proxy to wt curli production. We detected no significant curli defects in the majority of mutants (30/40, or 75% [see Fig. S5 in the supplemental material]). These findings suggest that the majority of biofilm defects observed in the Tn mutants during growth in YESCA are not attributed to defective curli expression. Notably, of the 10 mutants with strikingly altered CR uptake, 6 belong to metabolic/cell maintenance processes (Tn::*pgm*, Tn::*greB*, Tn::*rrsH*, Tn::*ygeX*, Tn::*mdh*, and Tn::*carB*), while 3 (Tn::*waaW*, Tn::*waaL*, and Tn::*cvpA*) belong to the LPS modification pathway or have hypothetical or uncharacterized functions. In addition to a defect in curli production, altered CR uptake may also point to a defect in cellulose or poly-β-1,6-*N*-acetyl-D-gluco-

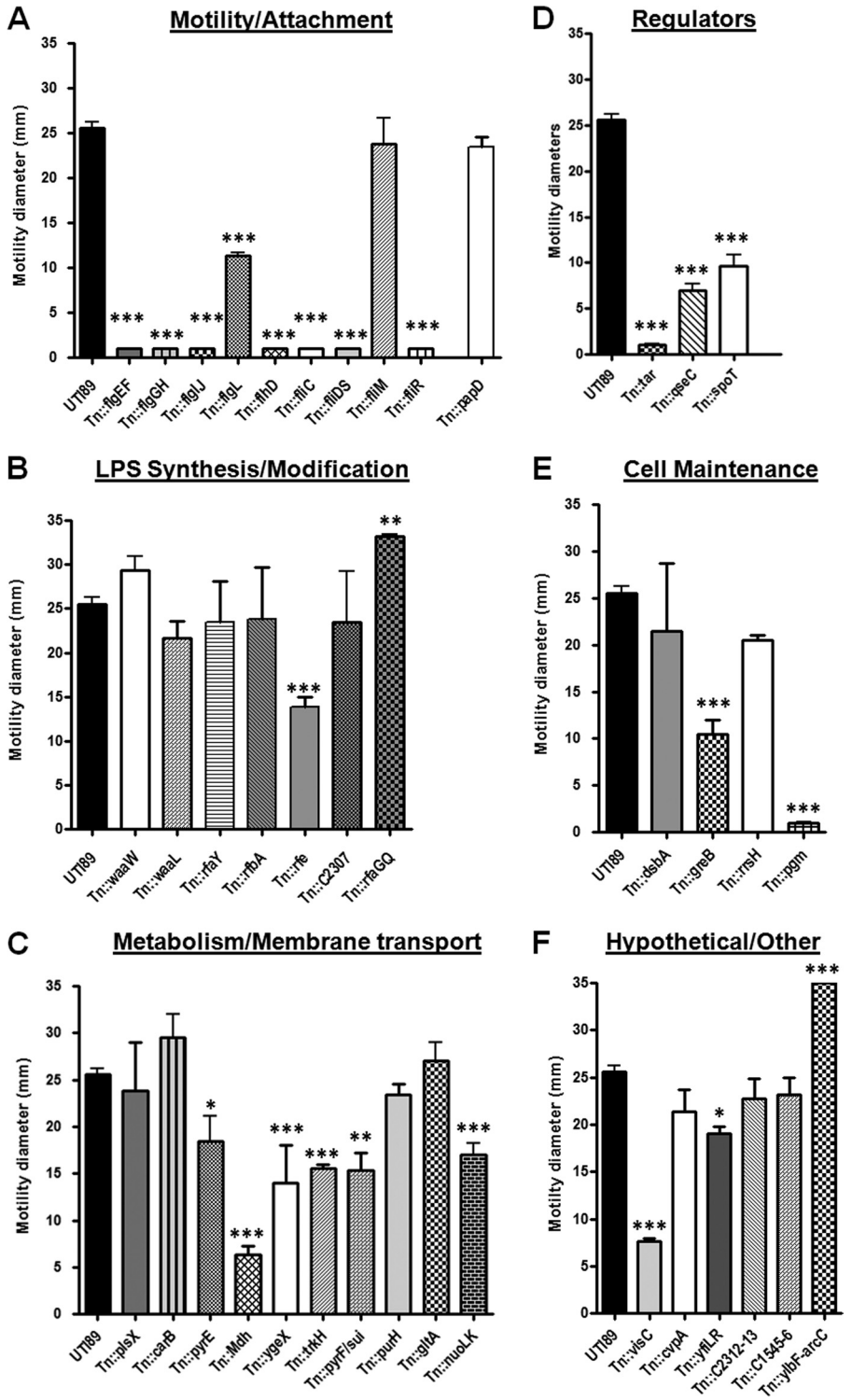

FIG 3 Motility properties of broad biofilm effectors. (A to F) Bar graphs depicting average motility diameters (in millimeters) of the different Tn mutants compared to the wt UTI89 after 7 h growth in soft LB agar (0.25%). Average motility diameters were calculated using data from 3 independent experiments. Statistical analyses were performed using unpaired, two-tailed Student's *t* test, with $P < 0.05$ considered significant. *, $P < 0.05$; **, $P < 0.005$; ***, $P < 0.0003$.

samine (PGA) production. Further analysis of these mutants will elucidate whether cellulose and PGA are perturbed.

Clustering analysis of mutants with generalized biofilm defects. Our *in vitro* assays probing for type 1 pili, curli, and flagella indicated that the majority of Tn mutants that had defects in all three biofilm conditions tested did not have significant defects in production of these organelles. To further investigate these results, we used a clustering approach to assess whether there were

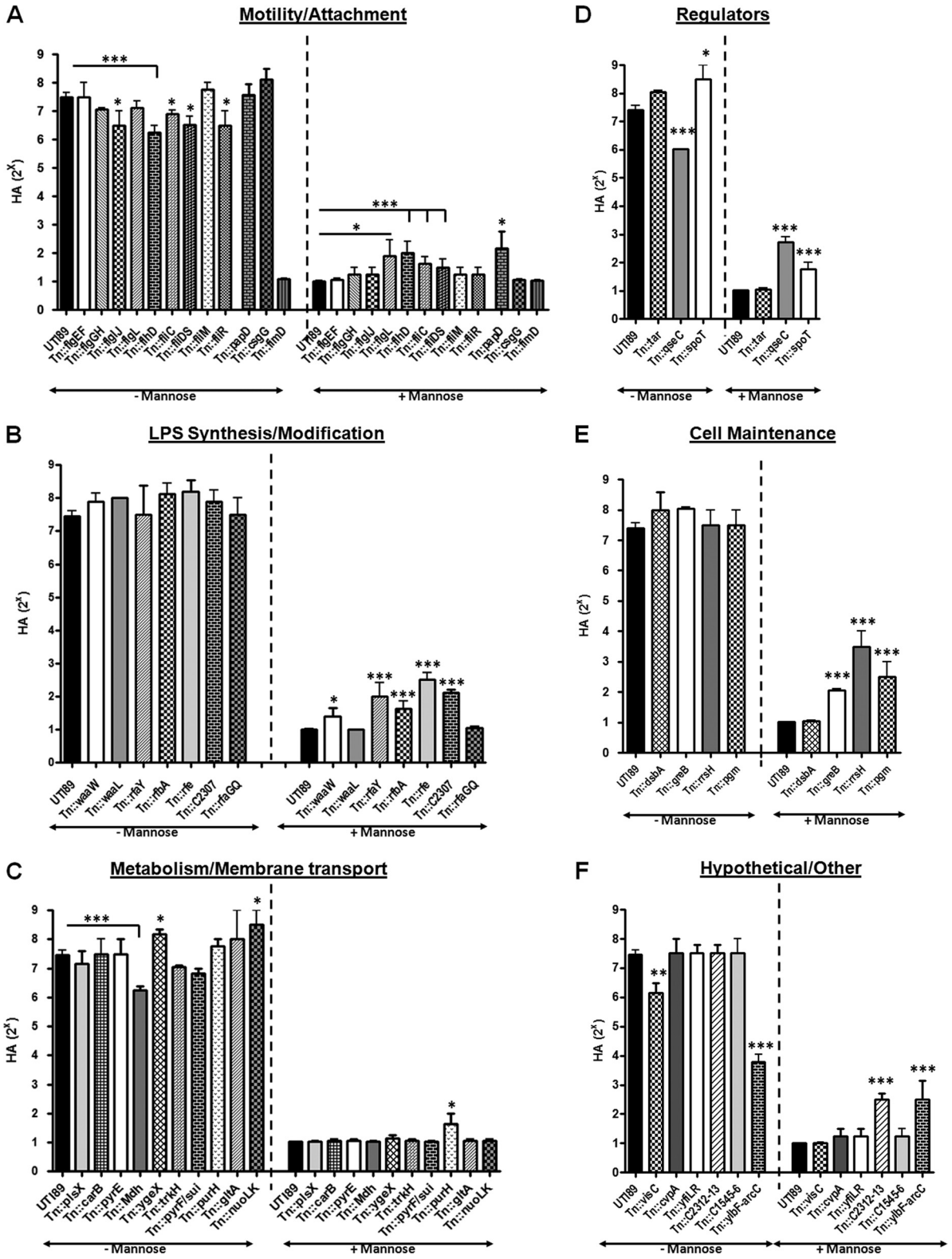

FIG 4 HA properties of broad biofilm effectors. (A to F) Bar graphs showing the HA properties of each Tn mutant compared to those of the wt UTI89 in the presence and absence of 4% D-mannose. Expression of type 1 pili can be evaluated by the ability of UPEC to agglutinate guinea pig red blood cells (RBCs) via recognition of mannosylated receptors by the FimH adhesin. The addition of mannose competitively inhibits type 1 pilus-mediated adhesion. Under the conditions tested, wt UTI89 typically expresses primarily type 1 pili; thus, the addition of mannose drops agglutination to an HA of 0 to 1. The small degree of agglutination remaining in the wt strain is attributable to some expression of S-pili. However, upon the addition of mannose, the HA of several Tn mutants did not drop to the typical 0 to 1, suggestive of additional pili systems that may be upregulated in these systems. The graphs depict average HA titers from 2 independent experiments. Statistical analyses were performed using unpaired, two-tailed Student's *t* test, with $P < 0.05$ considered significant. *, $P < 0.05$; **, $P < 0.005$; ***, $P < 0.0003$.

Locus	Gene Name	LB-PVC (%WT)	YESCA-PVC (%WT)	Pellicle Score (0-4, WT=4)	Motility diameter (WT=24-26mm)	MS-HA (WT=7-8 log 2	MR-HA (WT=0-1 log 2)	CR Uptake
UTI89_C4195	*spoT*	10	8	1	9.7	9	2	WT
UTI89_C3451	*qseC*	13	6.9	0	7	6	3	
UTI89_C0548-4	*ylbF-arcC*	18.3	95	2.5	35	4	4	WT
UTI89_C3813-1	purH-hypoth.	24.9	8.5	0	WT (25)	WT (8)	2	WT
UTI89_C1545-4	hypoth.	25	44	2	WT	WT	0	WT
UTI89_C1215	*plsX*	27.6	33.9	3	WT	WT	0	WT
UTI89_C3292	*visC*	27.8	163.3	3	7.7	6	0	WT
UTI89_C3667	*mdh*	41	28	0.5	6	6	0	
UTI89_C1552-3	pyrF-sui	43	24	1	16	WT	0	WT
UTI89_C2597	*cvpA*	45.3	26	0	WT	WT	0	
UTI89_C1208	*flgL*	65	10	1	11.5	WT	2.5	WT
UTI89_C0037	*carB*	65	63	1	WT	WT	0	
UTI89_C0692-0	*seqA-pgm*	68	14.9	1	0	WT	3	
UTI89_C4340	*rfe*	71.5	7	1	13.8	WT	3	WT
UTI89_C4434	*trkH*	75	22	1	16	WT	0	WT
UTI89_C0715-6	gltA	82	74	2.5	WT	WT	0	WT
UTI89_C2125-6	*fliD-S*	84	10	1	0	WT	2	WT
UTI89_C2095	*flhD*	84	34	1	0	6	2.5	WT
UTI89_C0217-8	*hypoth.*	85	9.3	1	20.5	WT	3.5	
UTI89_C1205-6	*flgI-J*	87	65	1.5	0	WT	0	WT
UTI89_C4186	*pyrE*	89.2	39	0	18	WT	0	WT
UTI89_C3255-5	ygeW-X	89.6	73.6	1	15	WT	0	
UTI89_C1203-0	*flgG-H*	93	30	1	0	WT	0	WT
UTI89_C4892	*papD*	93	39	1	WT	WT	2	WT
UTI89_C4170	*rfaY*	97	72	3	WT	WT	3	WT
UTI89_C2150	*fliR*	105	62	1	0	WT	0	WT
UTI89_C2125	*fliD*	107	32	2	0	WT	2	WT
UTI89_C2124	*fliC*	108	52	1	0	6.5	2	WT
UTI89_C2089	*tar*	110	55	>4	0	WT	0	WT
UTI89_C1371	*dsbA*	118.4	209	2.5	21.5	WT	0	WT
UTI89_C2635-6	*yfiL-R*	119	377	>4	19	WT	2	WT
UTI89_C3907	*greB*	130	21.6	1	10.5	WT	2	
UTI89_C2145	*fliM*	132	43.6	3	WT	WT	0	WT
UTI89_C1201-1	*flgE-F*	134.6	48.6	1	0	WT	0	WT
UTI89_C2312-1	*rfbB-hypoth.*	137.1	19.9	1	WT	WT	2.5	WT
UTI89_C3256	*ygeX*	138	10.4	0	16	WT	0	
UTI89_C2310	*rfbA*	140.6	36.9	1.5	WT	9	2	WT
UTI89_C4167	*waaL*	148.2	19.7	1	WT	WT	0	
UTI89_C2558-9	nuoL-K	150	19	3	17	9	0	WT
UTI89_C4169-7	*waaW-rfaY*	164	17	0.5	WT	9	2	
UTI89_C4169	*waaW*	177	37	0.5	WT	9	2	
UTI89_C2306-0	*wciP-hypoth.*	230	25.5	2	WT	WT	2	WT
UTI89_C4174-7	*rfaG-Q*	405	144	2.5	33.2	WT	0	WT

WT biomass*	50.1-75% WT	>175% WT	
*Architectural mutants with 85-115% of WT biomass also in this category	25.1-50% WT	150.1-175% WT	
	0-25% WT	125.1-150%WT	
		110-125% WT	

FIG 5 Clustering of broad biofilm mutant *in vitro* phenotypes. Mutants were clustered on the basis of phenotype severity; mutants were sorted by LB-PVC phenotype severity, followed by sorting based on the severity on YESCA-PVC, pellicle, motility, and CR uptake phenotypes. The colors indicate phenotype gain (green) or loss (red) compared to wt UTI89. In the biofilm value columns, the gray background denotes mutants with architectural biofilm defects that quantitatively produced 85% to 115% biomass compared to wt UTI89.

correlations between the pattern of biofilm phenotypes observed, based on quantitative biofilm defects under the three conditions tested, and the pattern of MS-HA, MR-HA, curli and flagellar phenotypes exhibited by each of the mutants. We first grouped all mutants based on biofilm severity and sorted them according to the effect of each mutation on the expression of type 1 pili (measured by MS-HA), curli (measured by CR uptake), or flagella (measured by motility). Architectural mutants with biofilm accumulation between 85% and 115% of the wild type were clustered as wt. Using this method, we discovered that most of the mutations that affected curli- and type 1-dependent biofilm formation did not always affect expression of those corresponding organelles. Thus, in these cases, these unique mutants may have led to the discovery of new factors that are important under these biofilm conditions. Also, loss or gain of motility did not strongly correlate with loss or gain of biofilm formation in the different mutants (Fig. 5). Specifically, we found that some nonmotile mutants had increased biofilm formation, while others exhibited strong biofilm defects (Fig. 5). These results have elucidated new genes and pathways possibly involved in initial adherence and intercellular aggregation, independent of type 1 pili, curli, and flagella, but which are important in type 1- and curli-dependent biofilms. Increased LB-PVC biofilm (Fig. 5, bottom quadrant) correlated with higher or wt levels of MS-HA (Fig. 5), but loss/reduction of LB-PVC biofilm did not have a strong correlation with reduced MS-HA (Fig. 5). Similarly, loss/reduction of CR uptake did not always correlate with reduced YESCA-PVC or pellicle biofilm (Fig. 5).

Taken together, these findings demonstrate that type 1 pili and curli are necessary but not sufficient for LB-PVC and YESCA-PVC/pellicle formation, respectively, and point toward other factors that are critical for proper biofilm formation under these conditions. In addition, the fact that these mutants express wt levels of type 1 pili and flagella, both of which have been extensively associated with initial adherence (38, 52, 55), supports the idea that the disrupted factors are corequisites for biofilm formation or may be involved at a stage in biofilm formation that is likely after initial adherence. Further studies investigating the stage at

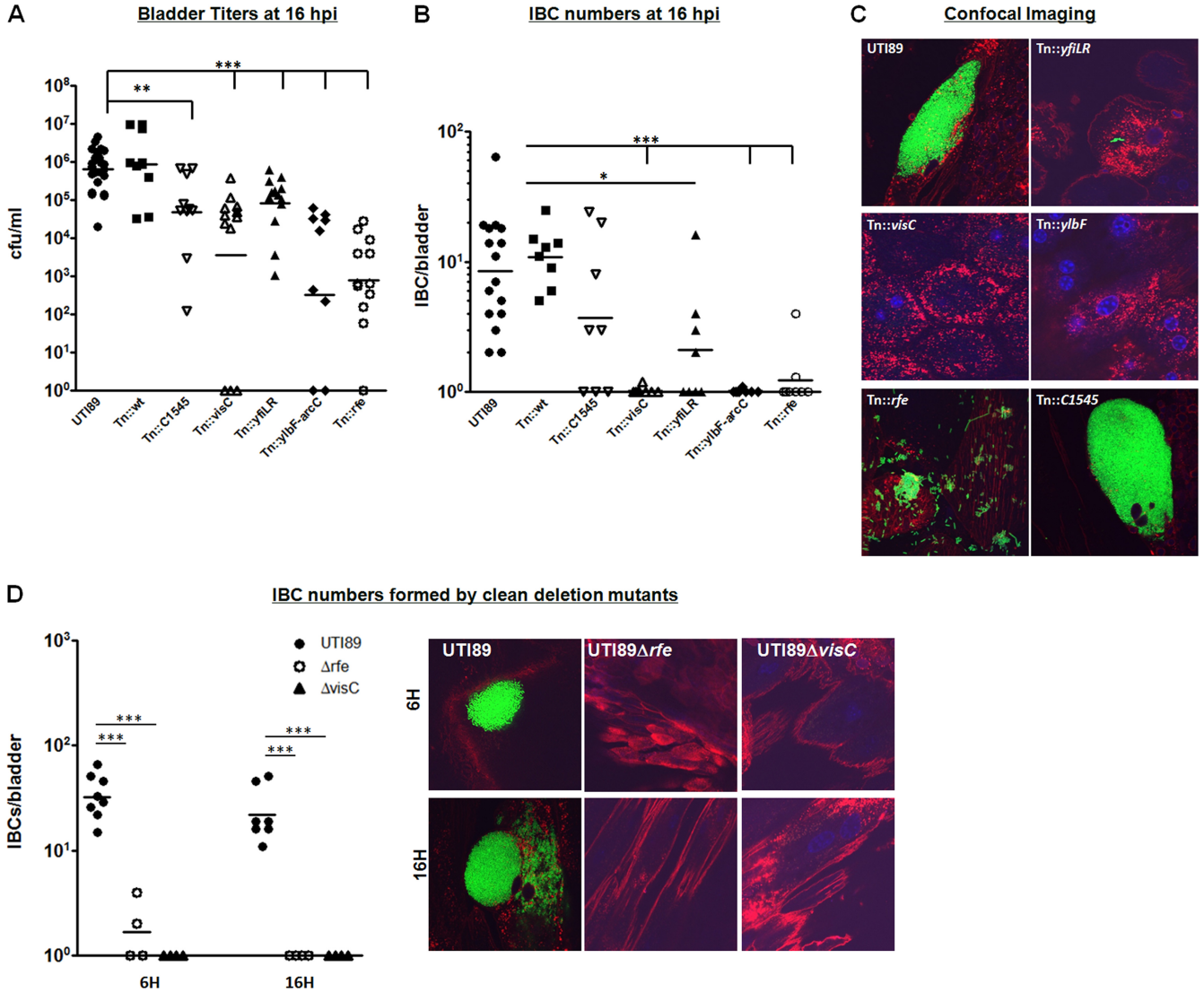

FIG 6 Hypothetical protein biofilm mutants are defective *in vivo*. (A and B) Graphs showing bladder titers (A) and IBC numbers (B) recovered 16 hpi with each Tn mutant. IBCs were enumerated by confocal microscopy as described in Materials and Methods. A $P < 0.01$ was considered significant by two-tailed Mann-Whitney test. (C) Confocal images (63×) depicting the bladder epithelial surface from mice infected with wt UTI89 or the corresponding Tn mutants. Bladder tissue is stained with wheat germ agglutinin (red), nuclei are stained with ToPro-3 iodide (blue), and UPEC are expressing GFP (green). A representative image is shown for each mutant. The experiment was repeated 3 times, and 5 bladders per mutant tested were imaged per experiment. (D) Graph and confocal imaging depicting IBC numbers enumerated for the corresponding UTI89Δ*visC* and UTI89Δ*rfe* nonpolar deletion mutants, both at 6 h and 16 h postinfection. The experiment was repeated twice. A *P* of <0.01 was considered significant by the two-tailed Mann-Whitney test. *, $P < 0.05$; **, $P < 0.005$; ***, $P < 0.0003$.

which these factors become important will provide more insights into the mechanisms that underlie multicellularity under the conditions tested.

Type 1 pilus-independent *in vivo* fitness defects in UTI. The role of biofilm determinants other than type 1 pili in IBC formation is largely unknown. Thus, we tested the *in vivo* fitness of a panel of Tn mutants (Tn::*visC*, Tn::*ylbF-arcC*, Tn::C1545-46, Tn::*yfiLR*, and Tn::*rfe* mutants) that exhibited a variety of biofilm defects and type 1 piliation phenotypes from wt to nonpiliated on the basis of the results of MS-HA and Western blot analysis (Fig. 5; see Fig. S2 in the supplemental material). Female C3H/HeN mice were then transurethrally inoculated with 10^7 CFU GFP-expressing strains of UTI89 or Tn::*visC*, Tn::*yfiLR*, Tn::C_1545-46, Tn::*ylbF-arcC*, and Tn::*rfe* mutant strains, The Tn::wt mutant, a transposon mutant with no biofilm defects, was included to control for any transposon-mediated effects. Bladder CFU and IBC numbers were monitored at 16 h postinfection (hpi), marking the end of the first IBC cycle at which time bacteria are found in late-stage IBCs or in the process of filamentation and dispersal (31). IBCs were enumerated by confocal microscopy as described previously (37). As expected, the Tn::wt strain colonized the bladder and formed IBCs at levels comparable to those of the wt UTI89 (Fig. 6A to C). All Tn mutants tested had at least 10-fold-lower bladder titers compared to wt UTI89 (Fig. 6A) and formed significantly fewer IBCs (Fig. 6B and C), with the exception of the Tn::C1545-46 mutant. The Tn::*rfe* mutant appeared to be mostly extracellular (Fig. 6C), with very few IBCs observed at 16 h postinfection. In order to validate these observations, we used two clean deletion

mutants that had different effects on type 1 pilus expression: UTI89Δ*visC* (reduced type 1 pili) and UTI89Δ*rfe* (no effects on type 1 pili expression). Introduction of these clean deletion mutants in mice and monitoring of CFU and IBC formation revealed that both mutants were significantly impaired in their ability to form IBCs (Fig. 6D), consistent with the results obtained using the transposon mutants. These observations are striking in that we have now discovered a panel of UPEC factors that affect IBC formation independent of type 1 pilus expression and when mutated attenuate virulence. Further analysis of such type 1 piliated mutants, such as UTI89Δ*rfe*, will uncover their specific roles in UPEC biofilm formation *in vitro* and *in vivo*. We are currently investigating these and other nonpolar clean deletion mutants further.

Concluding remarks. Collectively, our studies have elucidated an inventory of UPEC factors that impact biofilm formation either by interfering with known, critical biofilm determinants or by yet uncharacterized mechanisms. *In vivo* analysis using a murine model of acute cystitis revealed that a randomly selected panel of biofilm mutants with variable defects in type 1 pilus expression was equally attenuated in their ability to cause infection and form IBCs. These factors not only constitute potential drug target candidates for antibiofilm therapeutics but can be extensively utilized as molecular scalpels for extending the characterization of biofilm development. Further analysis of the pathways to which all these novel factors belong will elucidate molecular mechanisms involved in UPEC biofilm formation *in vitro* and *in vivo* and will advance our efforts in preventing or disassembling UPEC biofilms within the host.

ACKNOWLEDGMENTS

We thank Sarah Pinkner for providing technical assistance with screening the transposon library. We are grateful to Thomas Hannan, Matthew Conover, and Michael Hibbing for critical review of the manuscript.

This work was supported by the Morse-Berg fellowship (to M.H.) and NIH grants P50 DK64540-010 and R01 AI02954921 (to S.J.H.).

REFERENCES

1. **Aberg A, Shingler V, Balsalobre C.** 2008. Regulation of the fimB promoter: a case of differential regulation by ppGpp and DksA in vivo. Mol. Microbiol. **67**:1223–1241.
2. **Abraham JM, Freitag CS, Clements JR, Eisenstein BI.** 1985. An invertible element of DNA controls phase variation of type 1 fimbriae of Escherichia coli. Proc. Natl. Acad. Sci. U. S. A. **82**:5724–5727.
3. **Anderson GG, Goller CC, Justice S, Hultgren SJ, Seed PC.** 2010. Polysaccharide capsule and sialic acid-mediated regulation promote biofilm-like intracellular bacterial communities during cystitis. Infect. Immun. **78**:963–975.
4. **Anderson GG, Martin SM, Hultgren SJ.** 2004. Host subversion by formation of intracellular bacterial communities in the urinary tract. Microbes Infect. **6**:1094–1101.
5. **Anderson GG, et al.** 2003. Intracellular bacterial biofilm-like pods in urinary tract infections. Science **301**:105–107.
6. **Anriany Y, Sahu SN, Wessels KR, McCann LM, Joseph SW.** 2006. Alteration of the rugose phenotype in waaG and ddhC mutants of Salmonella enterica serovar Typhimurium DT104 is associated with inverse production of curli and cellulose. Appl. Environ. Microbiol. **72**:5002–5012.
7. **Barnhart MM, Chapman MR.** 2006. Curli biogenesis and function. Annu. Rev. Microbiol. **60**:131–147.
8. **Beloin C, et al.** 2006. The transcriptional antiterminator RfaH represses biofilm formation in Escherichia coli. J. Bacteriol. **188**:1316–1331.
9. **Bian Z, Brauner A, Li Y, Normark S.** 2000. Expression of and cytokine activation by Escherichia coli curli fibers in human sepsis. J. Infect. Dis. **181**:602–612.
10. **Bishop BL, et al.** 2007. Cyclic AMP-regulated exocytosis of Escherichia coli from infected bladder epithelial cells. Nat. Med. **13**:625–630.
11. **Blango MG, Mulvey MA.** 2010. Persistence of uropathogenic Escherichia coli in the face of multiple antibiotics. Antimicrob. Agents Chemother. **54**:1855–1863.
12. **Bouckaert J, et al.** 2005. Receptor binding studies disclose a novel class of high-affinity inhibitors of the Escherichia coli FimH adhesin. Mol. Microbiol. **55**:441–455.
13. **Bryan A, et al.** 2006. Regulation of type 1 fimbriae by unlinked FimB- and FimE-like recombinases in uropathogenic Escherichia coli strain CFT073. Infect. Immun. **74**:1072–1083.
14. **Buckles EL, et al.** 2004. Identification and characterization of a novel uropathogenic Escherichia coli-associated fimbrial gene cluster. Infect. Immun. **72**:3890–3901.
15. **Cegelski L, Pinkner JS, et al.** 2009. Small-molecule inhibitors target Escherichia coli amyloid biogenesis and biofilm formation. Nat. Chem. Biol. **5**:913–919.
16. **Chen SL, et al.** 2006. Identification of genes subject to positive selection in uropathogenic strains of Escherichia coli: a comparative genomics approach. Proc. Natl. Acad. Sci. U. S. A. **103**:5977–5982.
17. **Cormack BP, Valdivia RH, Falkow S.** 1996. FACS-optimized mutants of the green fluorescent protein (GFP). Gene **173**:33–38.
18. **Dodson KW, et al.** 2001. Structural basis of the interaction of the pyelonephritic E. coli adhesin to its human kidney receptor. Cell **105**:733–743.
19. **Domka J, Lee J, Bansal T, Wood TK.** 2007. Temporal gene expression in Escherichia coli K-12 biofilms. Environ. Microbiol. **9**:332–346.
20. **Eto DS, Jones TA, Sundsbak JL, Mulvey MA.** 2007. Integrin-mediated host cell invasion by type 1-piliated uropathogenic Escherichia coli. PLoS Pathog. **3**:e100. doi:10.1371/journal.ppat.0030100.
21. **Ferrieres L, Hancock V, Klemm P.** 2007. Biofilm exclusion of uropathogenic bacteria by selected asymptomatic bacteriuria Escherichia coli strains. Microbiology **153**:1711–1719.
22. **Garofalo CK, et al.** 2007. Escherichia coli from urine of female patients with urinary tract infections is competent for intracellular bacterial community formation. Infect. Immun. **75**:52–60.
23. **Goryshin IY, Jendrisak J, Hoffman LM, Meis R, Reznikoff WS.** 2000. Insertional transposon mutagenesis by electroporation of released Tn5 transposition complexes. Nat. Biotechnol. **18**:97–100.
24. **Griebling TL.** 2007. Urinary tract infection in women, p 589–617. *In* Litwin MS, Saigal CS (ed), Urologic diseases in America. NIH publication 07-5512. National Institute of Diabetes and Digestive and Kidney Disease, National Institutes of Health, Bethesda, MD.
25. **Hadjifrangiskou M, et al.** 2011. A central metabolic circuit controlled by QseC in pathogenic Escherichia coli. Mol. Microbiol. **80**:1516–1529.
26. **Hannan TJ, et al.** 2008. LeuX tRNA-dependent and -independent mechanisms of Escherichia coli pathogenesis in acute cystitis. Mol. Microbiol. **67**:116–128.
27. **Hasman H, Chakraborty T, Klemm P.** 1999. Antigen-43-mediated autoaggregation of Escherichia coli is blocked by fimbriation. J. Bacteriol. **181**:4834–4841.
28. **Henderson JP, et al.** 2009. Quantitative metabolomics reveals an epigenetic blueprint for iron acquisition in uropathogenic Escherichia coli. PLoS Pathog. **5**:e1000305. doi:10.1371/journal.ppat.1000305.
29. **Hultgren SJ, Schwan WR, Schaeffer AJ, Duncan JL.** 1986. Regulation of production of type 1 pili among urinary tract isolates of Escherichia coli. Infect. Immun. **54**:613–620.
30. **Hung CS, et al.** 2002. Structural basis of tropism of Escherichia coli to the bladder during urinary tract infection. Mol. Microbiol. **44**:903–915.
31. **Justice SS, et al.** 2004. Differentiation and developmental pathways of uropathogenic Escherichia coli in urinary tract pathogenesis. Proc. Natl. Acad. Sci. U. S. A. **101**:1333–1338.
32. **Kai-Larsen Y, et al.** 2010. Uropathogenic Escherichia coli modulates immune responses and its curli fimbriae interact with the antimicrobial peptide LL-37. PLoS Pathog. **6**:e1001010. doi:10.1371/journal.ppat.1001010.
33. **Kau AL, Hunstad DA, Hultgren SJ.** 2005. Interaction of uropathogenic Escherichia coli with host uroepithelium. Curr. Opin. Microbiol. **8**:54–59.
34. **Klemm P.** 1986. Two regulatory fim genes, fimB and fimE, control the phase variation of type 1 fimbriae in Escherichia coli. EMBO J. **5**:1389–1393.
35. **Kline KA, Dodson KW, Caparon MG, Hultgren SJ.** 2010. A tale of two pili: assembly and function of pili in bacteria. Trends Microbiol. **18**:224–232.
36. **Korhonen TK, et al.** 1984. Escherichia coli fimbriae recognizing sialyl galactosides. J. Bacteriol. **159**:762–766.

37. **Kostakioti M, Hadjifrangiskou M, Pinkner JS, Hultgren SJ.** 2009. QseC-mediated dephosphorylation of QseB is required for expression of genes associated with virulence in uropathogenic Escherichia coli. Mol. Microbiol. **73**:1020–1031.
38. **Landini P, Zehnder AJ.** 2002. The global regulatory hns gene negatively affects adhesion to solid surfaces by anaerobically grown Escherichia coli by modulating expression of flagellar genes and lipopolysaccharide production. J. Bacteriol. **184**:1522–1529.
39. **Lane MC, Alteri CJ, Smith SN, Mobley HL.** 2007. Expression of flagella is coincident with uropathogenic Escherichia coli ascension to the upper urinary tract. Proc. Natl. Acad. Sci. U. S. A. **104**:16669–16674.
40. **Lane MC, Simms AN, Mobley HL.** 2007. Complex interplay between type 1 fimbrial expression and flagellum-mediated motility of uropathogenic Escherichia coli. J. Bacteriol. **189**:5523–5533.
41. **Lenz AP, Williamson KS, Pitts B, Stewart PS, Franklin MJ.** 2008. Localized gene expression in Pseudomonas aeruginosa biofilms. Appl. Environ. Microbiol. **74**:4463–4471.
42. **Lewis K.** 2005. Persister cells and the riddle of biofilm survival. Biochemistry (Mosc.) **70**:267–274.
43. **Martinez JJ, Mulvey MA, Schilling JD, Pinkner JS, Hultgren SJ.** 2000. Type 1 pilus-mediated bacterial invasion of bladder epithelial cells. EMBO J. **19**:2803–2812.
44. **Monds RD, O'Toole GA.** 2009. The developmental model of microbial biofilms: ten years of a paradigm up for review. Trends Microbiol. **17**: 73–87.
45. **Morschhauser J, Vetter V, Korhonen T, Uhlin BE, Hacker J.** 1993. Regulation and binding properties of S fimbriae cloned from E. coli strains causing urinary tract infection and meningitis. Zentralbl. Bakteriol. **278**: 165–176.
46. **Mulvey MA, et al.** 1998. Induction and evasion of host defenses by type 1-piliated uropathogenic Escherichia coli. Science **282**:1494–1497.
47. **Mulvey MA, Schilling JD, Hultgren SJ.** 2001. Establishment of a persistent Escherichia coli reservoir during the acute phase of a bladder infection. Infect. Immun. **69**:4572–4579.
48. **Mulvey MA, Schilling JD, Martinez JJ, Hultgren SJ.** 2000. Bad bugs and beleaguered bladders: interplay between uropathogenic Escherichia coli and innate host defenses. Proc. Natl. Acad. Sci. U. S. A. **97**:8829–8835.
49. **Murphy KC, Campellone KG.** 2003. Lambda Red-mediated recombinogenic engineering of enterohemorrhagic and enteropathogenic E. coli. BMC Mol. Biol. **4**:11. doi:10.1186/1471-2199-4-11.
50. **Mysorekar IU, Hultgren SJ.** 2006. Mechanisms of uropathogenic Escherichia coli persistence and eradication from the urinary tract. Proc. Natl. Acad. Sci. U. S. A. **103**:14170–14175.
51. **O'Toole G, Kaplan HB, Kolter R.** 2000. Biofilm formation as microbial development. Annu. Rev. Microbiol. **54**:49–79.
52. **O'Toole GA, et al.** 1999. Genetic approaches to study of biofilms. Methods Enzymol. **310**:91–109.
53. **Parsek MR, Singh PK.** 2003. Bacterial biofilms: an emerging link to disease pathogenesis. Annu. Rev. Microbiol. **57**:677–701.
54. **Pinkner JS, et al.** 2006. Rationally designed small compounds inhibit pilus biogenesis in uropathogenic bacteria. Proc. Natl. Acad. Sci. U. S. A. **103**:17897–17902.
55. **Pratt LA, Kolter R.** 1998. Genetic analysis of Escherichia coli biofilm formation: roles of flagella, motility, chemotaxis and type I pili. Mol. Microbiol. **30**:285–293.
56. **Prigent-Combaret C, et al.** 2001. Complex regulatory network controls initial adhesion and biofilm formation in Escherichia coli via regulation of the csgD gene. J. Bacteriol. **183**:7213–7223.
57. **Rosen DA, Hooton TM, Stamm WE, Humphrey PA, Hultgren SJ.** 2007. Detection of intracellular bacterial communities in human urinary tract infection. PLoS Med. **4**:e329. doi:10.1371/journal.pmed.0040329.
58. **Schembri MA, Dalsgaard D, Klemm P.** 2004. Capsule shields the function of short bacterial adhesins. J. Bacteriol. **186**:1249–1257.
59. **Schwan WR.** 2008. Flagella allow uropathogenic Escherichia coli ascension into murine kidneys. Int. J. Med. Microbiol. **298**:441–447.
60. **Schwartz DJ, Chen SL, Hultgren SJ, Seed PC.** 2011. Population dynamics and niche distribution of uropathogenic Escherichia coli during acute and chronic urinary tract infection. Infect. Immun. **79**:4250–4259.
61. **Song J, et al.** 2009. TLR4-mediated expulsion of bacteria from infected bladder epithelial cells. Proc. Natl. Acad. Sci. U. S. A. **106**:14966–14971.
62. **Thankavel K, et al.** 1997. Localization of a domain in the FimH adhesin of Escherichia coli type 1 fimbriae capable of receptor recognition and use of a domain-specific antibody to confer protection against experimental urinary tract infection. J. Clin. Invest. **100**:1123–1136.
63. **Thumbikat P, et al.** 2009. Bacteria-induced uroplakin signaling mediates bladder response to infection. PLoS Pathog. **5**:e1000415. doi:10.1371/journal.ppat.1000415.
64. **Uhlin BE, Norgren M, Baga M, Normark S.** 1985. Adhesion to human cells by Escherichia coli lacking the major subunit of a digalactoside-specific pilus-adhesin. Proc. Natl. Acad. Sci. U. S. A. **82**:1800–1804.
65. **Ulett GC, Webb RI, Schembri MA.** 2006. Antigen-43-mediated autoaggregation impairs motility in Escherichia coli. Microbiology **152**:2101–2110.
66. **Vuong C, et al.** 2004. Polysaccharide intercellular adhesin (PIA) protects Staphylococcus epidermidis against major components of the human innate immune system. Cell. Microbiol. **6**:269–275.
67. **Waksman G, Hultgren SJ.** 2009. Structural biology of the chaperone-usher pathway of pilus biogenesis. Nat. Rev. Microbiol. **7**:765–774.
68. **Warren JW.** 2001. Catheter-associated urinary tract infections. Int. J. Antimicrob. Agents **17**:299–303.
69. **Wiles TJ, Kulesus RR, Mulvey MA.** 2008. Origins and virulence mechanisms of uropathogenic Escherichia coli. Exp. Mol. Pathol. **85**:11–19.
70. **Wright KJ, Seed PC, Hultgren SJ.** 2007. Development of intracellular bacterial communities of uropathogenic Escherichia coli depends on type 1 pili. Cell. Microbiol. **9**:2230–2241.
71. **Wright KJ, Seed PC, Hultgren SJ.** 2005. Uropathogenic Escherichia coli flagella aid in efficient urinary tract colonization. Infect. Immun. **73**:7657–7668.
72. **Xie B, et al.** 2006. Distinct glycan structures of uroplakins Ia and Ib: structural basis for the selective binding of FimH adhesin to uroplakin Ia. J. Biol. Chem. **281**:14644–14653.
73. **Zhou G, et al.** 2001. Uroplakin Ia is the urothelial receptor for uropathogenic Escherichia coli: evidence from in vitro FimH binding. J. Cell Sci. **114**:4095–4103.